Polymer Chemistry

ROYAL SOCIETY OF CHEMISTRY

PAPER

View Article Online
View Journal | View Issue

Cite this: *Polym. Chem.*, 2024, **15**, 4474

Simple oxime functionalized fluorene polymers for organic solar cells†

Abdullah Adewale Adeoba,[a,b] Xiangyu Shen,[a] Fuzhen Bi,[a] Jianan Niu,[a] Mingxin Sun,[c] Shuguang Wen *[a,b] and Xichang Bao *[a,b]

Received 22nd August 2024,
Accepted 11th October 2024

DOI: 10.1039/d4py00919c

rsc.li/polymers

Conjugated polymers with simple chemical structures are attractive for the design of high efficiency, wide bandgap (WBG) donor materials used in non-fullerene organic solar cells. Fluorene is one of the most common structures in organic opto-electronic materials. It is herein used, for the first time, functionalized with the oxime group to construct the acceptor unit of D–A polymer donors with a BDT donor unit. The polymers, PBFO-H and PBFO-F, had low-lying HOMOs with a wide bandgap of 2.08 eV and are soluble in chloroform for easy processing. Organic solar cells were constructed using the polymers and a non-fullerene Y6 acceptor. The fluorinated polymer (PBFO-F) had better photovoltaic properties over the non-fluorinated polymer overall, with J_{SC}, V_{OC}, and FF values of 23.17 mA cm^{-2}, 0.84 V, and 55.2%, respectively, and a high PCE of 10.71%. These results demonstrate that fluorene is promising in constructing acceptor units for D–A wide bandgap polymers.

Introduction

Polymer solar cells (PSCs), otherwise known as organic solar cells (OSCs) have drawn scientific and commercial attention because of their numerous advantages.[1,2] This class of solar cells is flexible and light-weight, can be processed in low-cost solutions, and is suitable for roll-to-roll mass production.[1,3,4] Nowadays, PSCs usually take the structure of a bulk heterojunction (BHJ) in which the conjugated polymer donor is blended with a small molecule acceptor. Fullerene based acceptors were used in the past with a maximum power conversion efficiency (PCE) of around 11%.[5] Even though fullerene-based acceptors have good properties such as good solubility, good electron transport and high electron affinity, the fact that they absorb weakly in the visible region of the solar spectrum, have limited energy level tunability, and can easily decompose with long term use, limits their further applications. The discovery of non-fullerene acceptors has led to the improvement of the PCEs of polymer solar cells close to 20%.[6–9] This could be attributed to the balance between the open circuit voltage (V_{OC}) and short circuit density (J_{SC}) while the fill factor (FF) has achieved a significant increase when matched against fullerene based solar cells.

The conjugated polymer donor used in PSCs usually takes a donor–acceptor (D–A) alternating molecular structure. In order to maximize their performance, the D and A units must be carefully selected so that their absorption spectra and frontier molecular orbital energy levels can be suitably modified to match with the acceptor materials.[10–12] Moreover, non-fullerene acceptors (NFAs) usually need a wide band gap (WBG) polymer donor ($E_g \geq 1.8$ eV) in order to complement their narrow absorption range.[13] Benzodiothiophene (BDT) is commonly used to construct the D building block of the D–A polymer due to its appropriate electron-donating effect which is good for the E_{HOMO}, a large planar structure which helps in hole transport and a face-on molecular orientation of thin films.[14,15] On the other hand, the chemical structures which have electron-withdrawing groups such as 3-fluorothieno[3,4-*b*]thiophene-2-carboxylate (FC-TT), thieno[3,4-*c*]pyrrole-4,6-dione (TPD), benzo[1,2-*c*:4,5-*c*′]dithiophene-4,8-dione (BDD), difluorobenzo[1,2,3]triazole (FBTA), quinoxaline, and benzothiadiazole (BT) have been used as the A building blocks.[13,15] The results of the different BDT-acceptor combinations show that the acceptor molecules have noticeable effects on the optical performances of the resulting D–A polymers and by extension, the PCEs of the resulting PSCs.[16–20]

Fluorene based polymers were known to be initially used for light emitting diodes (LEDs) with absorption at short wavelengths.[21] The major advantages of the fluorene compounds include a highly conjugated ring, efficient hole transport, chemical stability, structural rigidity and planarity which give wide band gaps and low HOMO levels, directly leading to a

[a]*CAS Key Laboratory of Bio-Based Materials, Qingdao Institute of Bioenergy and Bioprocess Technology, China. E-mail: wensg@qibebt.ac.cn, baoxc@qibebt.ac.cn*
[b]*Functional Laboratory of Solar Energy, Shandong Energy Institute, Qingdao 266101, China*
[c]*Qingdao New Energy Shandong Laboratory, Qingdao 266101, China*
† Electronic supplementary information (ESI) available. See DOI: https://doi.org/10.1039/d4py00919c

high V_{OC} and J_{SC}.[16,22–24] It was later used to design polymer solar cell donor materials by Andersson and co-workers with the resulting PSC having a PCE of 2.2%. After this, many groups have introduced different side-chains into fluorene to improve its various photovoltaic parameters with PCEs of 3.5%,[25] 4.5%,[26] and 6.6%[27] when used for PSCs. It should be noted that in all of these studies, fluorene is used as the electron-donating unit while its application as the electron-accepting unit in a D–A polymer still remains unreported. Furthermore, fluorene units also feature simple and planar molecular structures, which would be suitable for the construction of efficient polymer donors for OSCs.

In this study, we introduce oxime-functionalized fluorine (FO) as an acceptor unit copolymerized with BDT monomers to synthesize two novel conjugated D–A donor polymers, PBFO-H and PBFO-F, which would be useful for OSCs.[28,29] The importance of the oxime functional group is due to its electron withdrawing ability and its usage in conjugated polymers is a fairly new concept, firstly used by He *et al.* on a thiophene-based monomer.[30] Therefore, this work effectively combines the novelty of fluorene as an acceptor unit and oxime as an electron withdrawing functional group. Molecular simulation shows that the fluorene unit is effective as an electron-withdrawing group. The introduction of the fluorine atom is efficient in modulating energy levels and most of its photovoltaic properties. The polymers have a wide bandgap (2.08 eV) and appropriate energy levels and thus were paired with the non-fullerene acceptor Y6 in constructing NFA polymer solar cells. A highest PCE value of 10.71% was obtained for the solar devices with the parameters J_{SC}, V_{OC} and E_{loss} approaching those of the state-of-the-art systems. These results show that fluorene would be a good choice for constructing the acceptor units in WBG D–A polymer donors for non-fullerene solar cells.

Results and discussion

Materials synthesis and characterization

The oxime-based fluorene monomer was synthesized from scratch as shown in Fig. 1. A hydroxylamine (**2**) was synthesized using a modification of methods used by Zhu *et al.*,[31] and Aldo *et al.*[32] with about 70% yield. The above was joined as an oxime functional group to a commercial 2,7-dibromo-9*H*-fluorene-9-one using a method reported by Blake *et al.*[33] A straight-chain alkylthiophene was further introduced through the Stille reaction process. Finally, the thiophenated compound (**4**) was brominated using *N*-bromosuccinimide to give the monomer M. The intermediates and final products were confirmed by nuclear magnetic resonance (NMR).

To get the polymers, the monomer M was copolymerized with BDT using $Pd(PPh_3)_4$ catalysts under Stille conditions. The two polymers synthesized, PBFO-H and PBFO-F, were both soluble in chloroform at room temperature, allowing for easy fabrication of the devices using a simple spin-coating method. The two polymers PBFO-H and PBFO-F have number-average molecular weights (M_n) of 121 and 35 kDa and PDI of 1.71 and 1.64 respectively, measured by high temperature gel permeation chromatography (GPC). The decomposition temperature (T_d, 5% weight loss) measured by thermogravimetric analysis (TGA) under a nitrogen atmosphere was 320 °C for PBFO-H and 240 °C for PBFO-F, indicating their good thermal stability for the fabrication of solar cells (Fig. S4†).

Optical properties and energy levels

The optical properties of the pair polymers were studied using ultraviolet-visible (UV-vis) spectroscopy and the results are shown in Fig. 2. The two polymers PBFO-H and PBFO-F in solution showed a low-energy peak of maximum absorption occurring at wavelengths of 477 nm and 505 nm (λ_{max}) respectively. Comparatively, PBFO-F shows a red-shifted absorption peak, and a shoulder peak can also be observed. This behavior indicates that PBFO-F has stronger aggregation tendency in solution than PBFO-H. The absorption spectra for both polymers in thin films are very similar, and PBFO-H has maximum absorption at 507 nm while PBFO-F has maximum absorption at 544 nm, on thin film. The occurrence of shoulder peaks in thin films could be attributed to improved polymer aggregation. The higher shoulder peak of PBFO-F implies its stronger aggregation behavior than PBFO-H, which would be induced

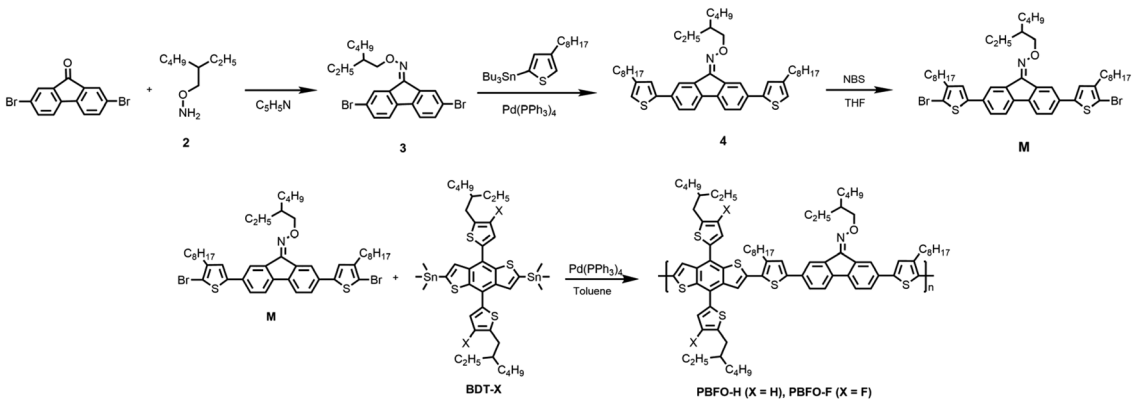

Fig. 1 Chemical structure and synthesis routes towards the monomer and polymers PBFO-H and PBFO-F.

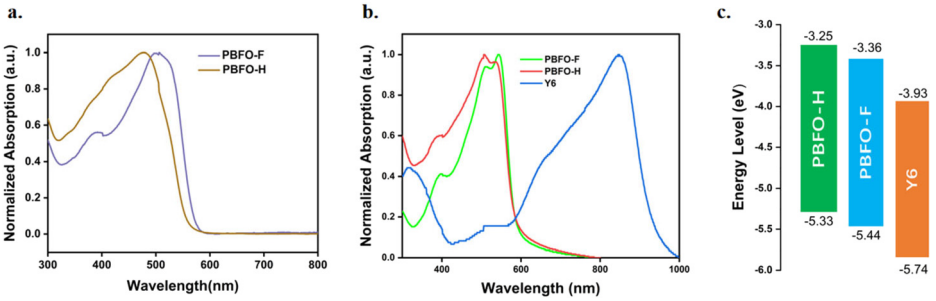

Fig. 2 (a) Normalized UV-vis absorption spectra of the polymers in dilute chloroform. (b) Normalized UV-vis absorption spectra of thin films. (c) Energy levels of PBFO-H, PBFO-F and Y6.

by the fluoride incorporated non-covalent bond interaction. The extinction coefficient (ϵ_{max}) for both polymers PBFO-H and PBFO-F are 3.91×10^4 cm^{-1} and 3.67×10^4 cm^{-1} for thin films at ~505 nm respectively, which are very close values due to their similar backbone. High extinction coefficient values would facilitate light harvesting in thin films (~100 nm), which is beneficial for efficient charge extraction while avoiding charge recombination. The optical bandgaps of the polymers in film, derived from the absorption onset is 2.08 eV for both polymers which is considered a wide bandgap. In conjunction with the strong absorption range of these polymers (400–544 nm), they are suitable for complementing non-fullerene acceptors (NFAs) due to their narrow bandgap absorption, for example, Y6, which absorbs between 600 and 930 nm and has E_g of 1.33 eV.[21] These pairs of polymers showed wider bandgaps when compared to a similar oxime-substituted polymer which used thiophene instead of a fluorene unit (E_g = 2.03 eV) which indicates that fluorene is more suitable for a wider bandgap due to the presence of more conjugation.[15]

Density functional theory (DFT) simulations were carried out at the B3LY/6-31G(d,p) level to understand the molecular geometries and electronic properties of the polymers. The alkyl side chains were replaced with methyl units to minimize computing time (Fig. S1†). The impact of the fluorine atom on the BDT unit is obviously noticed in delocalizing electrons across the backbone of the polymer. The polymer without the fluorine side chain (PBFO-H) has most of its HOMO electron cloud localized on the BDT unit while introducing fluorine helped to spread out the electron cloud throughout the polymer backbone as seen in PBFO-F, making it have a more planar chain which is advantageous for efficient charge transport. As for the LUMO electron cloud, it is majorly situated on the fluorene acceptor side chain which proves it as a novel effective electron-withdrawing unit. Some LUMO electron cloud could also be noticed on the oxime (=N–O) functional group which also proves its electron-withdrawing property. The HOMO/LUMO energy levels calculated for PBFO-H and PBFO-F were −4.94/−2.02 and −5.06/−2.09 eV respectively showing that the introduction of fluorine helps to deepen the HOMO level. The dihedral angles between thiophene and BDT units are 22.7° and 21.6° for PBFO-H and PBFO-F respectively, while the thiophene and fluorene molecules are joined at −24.5° and −26.4° for PBFO-H and −24.6° and −26.3° for PBFO-F. The small dihedral angles present in the polymers confirm the planarity which will enable ordered molecular packing and charge transport in devices.

The energy levels of the polymers were also investigated using cyclic voltammetry (CV) experiments (Fig. S2†), and the results are shown in Table 1. The HOMO/LUMO energy levels of polymers PBFO-H and PBFO-F were obtained to be −5.33/−3.25 eV and −5.44/−3.36 eV respectively. The effect of introducing fluorine into the polymer is clearly pronounced in reducing the LUMO level and deepening the HOMO level which is useful for it to approach the energy levels of the Y6 acceptor (−5.74/−3.93 eV) in order to reduce energy loss. The difference between the E_{HOMO} of the polymers and E_{LUMO} of Y6 is at least 1.4 eV, which would lead to high V_{OC} when blended together. The HOMO and LUMO energy offsets, ΔE_{HOMO} and ΔE_{LUMO} between the PBFO polymers and Y6 is in the least 0.30 eV and 0.57 eV respectively, sufficient enough for driving exciton dissociation.

Table 1 Optical, electrochemical and surface energy properties of the polymers

	λ_{max} [nm]						
Polymer	Solution	Film	λ_{onset} [nm]	E_g^{opt} [eV]	E_{HOMO}[a] [eV]	E_{LUMO}[b] [eV]	γ [mN m^{-1}]
PBFO-H	478	507	596	2.08	−5.33	−3.25	40.9
PBFO-F	505	544	597	2.08	−5.44	−3.36	43.4

[a] Measured by cyclic voltammetry measurement. [b] Calculated using $E_{LUMO} = E_{HOMO} + E_g^{opt}$.

Photovoltaic and electrical properties

Photovoltaic devices based on the glass/ITO (indium tin oxide)/PEDOT:PSS (poly(3,4-ethylenedioxythiophene):poly(styrenesulfonate))/active layer/PDINN (aliphatic amine-functionalized perylene-diimide)/Ag structure were constructed in order to evaluate the photovoltaic properties of the polymers. Y6 was used as the acceptor layer, blended together with the polymers to form the active layers. The current density–voltage (J–V) graph of the optimized devices with a donor/acceptor ratio of 1 : 1 is shown in Fig. 3a and the photovoltaic properties are summarized in Table 2. A reference of the detailed device fabrication process is provided in the ESI (Tables S1 and S2†). The devices achieved maximum performances when they were optimized through the addition of 0.2% diiodooctane (DIO). Under these conditions, the PBFO-H:Y6 based device showed an efficiency of 7.26% with V_{OC} of 0.77 V, a fill factor of 47.38% and J_{SC} of 19.94 mA cm^{-2}. With fluorine atom introduced into the polymer donor backbone, the device based on PBFO-F:Y6 had a stellar efficiency of 10.71% with a V_{OC} value of 0.84 V, a J_{SC} value of 23.17 mA cm^{-2}, and an FF value of 55.2%. The simultaneous improvement of all the device parameters with the introduction of fluorine shows that it is an efficient strategy for improving the photovoltaic performance of the devices. The two devices based on PBFO-H and PBFO-F have V_{OC} values of 0.77 V and 0.84 V respectively, which translates to respective E_{loss} of 0.55 and 0.49 eV, computed from the equation $E_{loss} = E_g - V_{OC}$. The E_{loss} for the PBFO-F:Y6 device, 0.49 eV, is very close to the lowest energy loss found for OSCs.[34,35]

The devices have J_{SC} values of 19.94 and 23.17 mA cm^{-2} respectively with the high J_{SC} and V_{OC} value of the PBFO-F device approaching state-of-the-art values.[9,30] The experimental J_{SC} value is also very close to that which was derived from the EQE curve ($J_{calc.}$) (Fig. 3b), which confirms the integrity of the calculation results. The FF values recorded for the devices (0.47 and 0.55) are low compared to the highest reported values (~0.76) but can be further improved through the optimization of side chain engineering and film morphology with an expectant increase in the PCE.[15] To recall from the optical absorption spectra, the donor polymer is responsible for the short wavelength absorption below 600 nm while the longer wavelength above 600 nm reflects the Y6 acceptor absorption. The EQE values in the shorter wavelength region are observed to be conspicuously higher than EQE values in the longer wavelength region which implies that the charges generated through photo-induced electron-transfer from the donor contributes more to the total efficient charges generated in the system.[36] This phenomenon brings to light

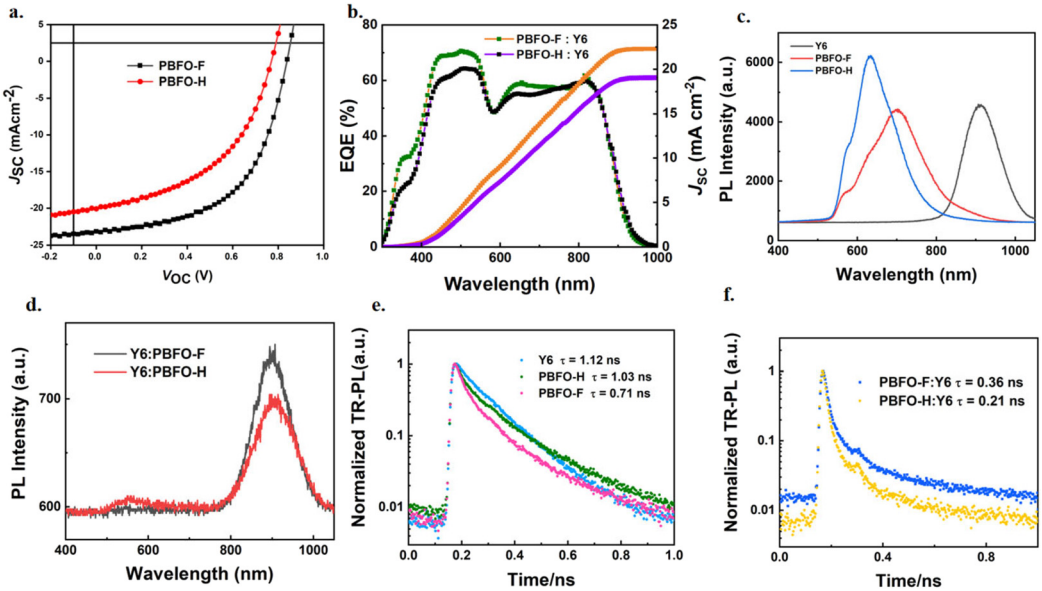

Fig. 3 (a) J–V curves and (b) the corresponding EQE spectra of the OSCs based on the polymer:Y6 (c) PL spectra of Y6, PBFO-F and PBFO-H (d) PL spectra of Y6:PBFO-F and Y6:PBFO-H devices (e) TRPL spectra of Y6, PBFO-F and PBFO-H and (f) TRPL spectra of PBFO-F:Y6 and PBFO-H:Y6.

Table 2 Photovoltaic parameters of OSCs under illumination of AM 1.5G, 100 mW cm^{-2}

Device	V_{OC} [V]	J_{SC} [mA cm^{-2}]	$J_{calc.}$[a] [mA cm^{-2}]	FF [%]	PCE[b] [%]	E_{loss}[c] [eV]
PBFO-H:Y6	0.77	19.94	19.06	47.38	7.26 (6.85 ± 0.40)	0.55
PBFO-F:Y6	0.84	23.17	22.28	55.20	10.71 (10.50 ± 0.26)	0.49

[a] Calculated from EQE curves. [b] The values are averages from 10 separate devices. [c] $E_{loss} = E_g - eV_{OC}$.

the potency of the fluorine-oxime (FO) acceptor building block used in the construction of the D–A donor polymer.

The exciton diffusion and dissociation properties of the devices were studied using photoluminescence (PL) and time-resolved photoluminescence (TRPL) spectra of neat and blend films with excitation at a wavelength of 400 nm. The results based on Fig. 3c and d show that blending the polymer and acceptor Y6 together reduced the emission of both the polymers and the Y6 acceptor. High quenching efficiencies were achieved for both PBFO-F:Y6 and PBFO-H:Y6 systems (83.3 and 88.3% respectively). It is observed that the PL intensity of PBFO-F:Y6 is more quenched in the donor region and enhanced in the acceptor region compared to that of PBFO-H:Y6, indicating more efficient charge separation between the donor and the acceptor. The fluorescence lifetime (τ) obtained from the TRPL spectra (Fig. 3e) was 1.12 ns for Y6, 1.03 ns for PBFO-F, and 0.71 ns for PBFO-H. On blending the polymers with the acceptor Y6, the lifetime of the PBFO-F:Y6 blend reduced to 0.36 ns while that of PBFO-H decreased to 0.21 ns (Fig. 3f) which is consistent with the PL results. The longer life time of the PBFO-F:Y6 blend is beneficial for excitons to diffuse and dissociate appropriately at the D–A interface in the blend, thus achieving higher J_{SC} and FF values.

Furthermore, the exciton dissociation and charge collection efficiencies of the system were investigated. The result, shown in Fig. 4a is a plot of photocurrent density (J_{ph}) against the effective applied voltage (V_{eff}). J_{ph} is associated with the current densities under illuminated (J_L) and dark conditions (J_D) according to the equation $J_{ph} = J_L - J_D$. V_{eff} is defined as $V_{eff} = V_0 - V_{appl}$, where V_0 is the voltage at which J_{ph} is 0 while V_{appl} is the applied voltage. As V_{eff} increases to unity, J_{ph} for PBFO-H:Y6 reaches a maximum value (J_{sat}) of 21.60 mA cm^{-2} under lower bias conditions while that of PBFO-F:Y6 reached 21.70 mA cm^{-2}. The exciton dissociation (η_{diss}) efficiencies which is calculated from J_{ph}/J_{sat} at the short-circuit current is found to be 93.9% and 95.5% for PBFO-H and PBFO-F respectively. On the other hand, the charge collection efficiencies (η_{coll}) for the devices calculated at the maximum power output point was found to be 63.0% for PBFO-H and 70.0% for PBFO-F. The PBFO-F based device shows higher η_{diss}/η_{coll} values than PBFO-H, which is consistent with the tendency of the FF values.

The light intensity (P_{light}) dependent J_{SC} and V_{OC} of the devices were used in analyzing their charge recombination properties. J_{SC} is proportional to an exponential of the light intensity defined by $J_{SC} \propto P_{light}^{\alpha}$ wherein the exponential factor (α) is usually close to 1 under short-circuit conditions since most of the photo-generated charges are evicted from the device and bimolecular recombination would be negligible.[37] As shown in Fig. 4b, the exponential factors (α) obtained for PBFO-H and PBFO-F are 0.95 and 0.99 respectively which corroborates with theory. Conversely, the light intensity dependent V_{OC} is usually measured under open circuit conditions, when no current is applied, to ensure that all photo-induced charges effectively recombine. The dependence of V_{OC} on P_{light} is governed by the equation $V_{OC} \propto (nkT/q) \times \ln(P_{light})$, where k is the Boltzmann constant, T is the temperature measured in Kelvin, and q is the elementary charge. The n parameter is usually close to 1 when only bimolecular recombination operates in the device but the trap-assisted recombination usually extends it to $1 < n < 2$.[38] The n value found for PBFO-F:Y6 (1.41) is to our surprise greater that of PBFO-H:Y6 (1.31), which signifies that PBFO-F is more affected by trap-assisted recombination, as shown in Fig. 4c. Space-charge limited current (SCLC) techniques were used to measure the hole-only and electron-only diodes in order to derive their hole and electron mobilities (μ_h and μ_e)

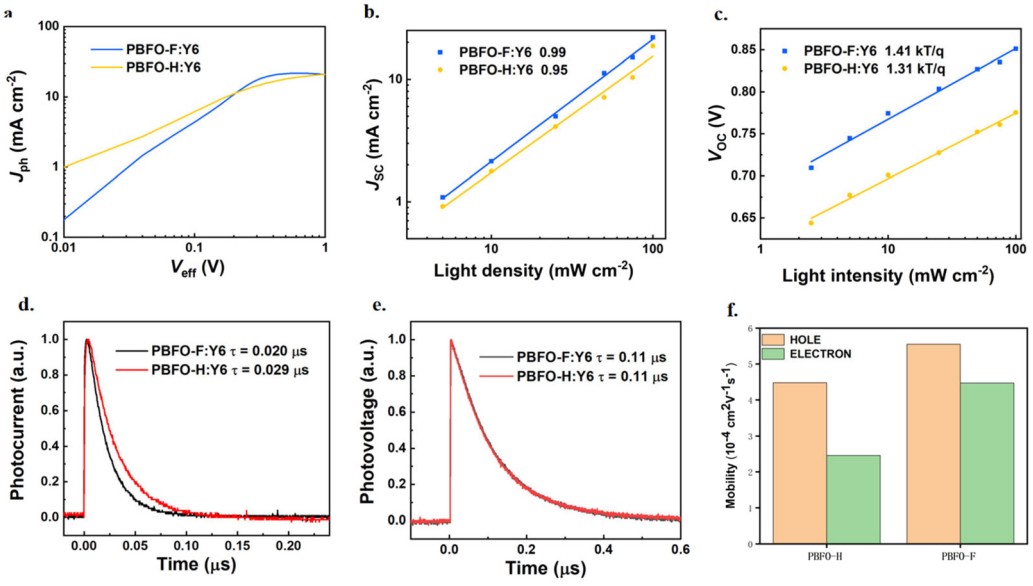

Fig. 4 (a) Photocurrent density (J_{ph}) against effective voltage (V_{eff}); dependence of (b) J_{SC} and (c) V_{OC} on P_{light} of the devices; (d) TPC curves; (e) TPV curves; and (f) charge mobility histogram.

respectively (Fig. S3 and Table S3†).[39] The μ_h and μ_e values of PBFO-F:Y6 are high at 5.55×10^{-4} cm^2 V^{-1} s^{-1} and 4.47×10^{-4} cm^2 V^{-1} s^{-1}, respectively, with a μ_h/μ_e ratio of 1.24 (Fig. 4f), suggesting that balanced μ_h and μ_e are achieved which is good for obtaining high J_{SC} and FF. On the other hand, the μ_h and μ_e values for the PBFO-H:Y6 blend are 4.48×10^{-4} cm^2 V^{-1} s^{-1} and 2.46×10^{-4} cm^2 V^{-1} s^{-1} with a μ_h/μ_e ratio of 1.82 which is more unbalanced compared with that of PBFO-F and would affect the J_{SC} negatively. These results demonstrate that the conjugated polymer based on oxime functionalized fluorene can achieve good charge mobility. The greater values in PBFO-F show that the addition of fluorine was effective in leading to better electron discharge and mobility.

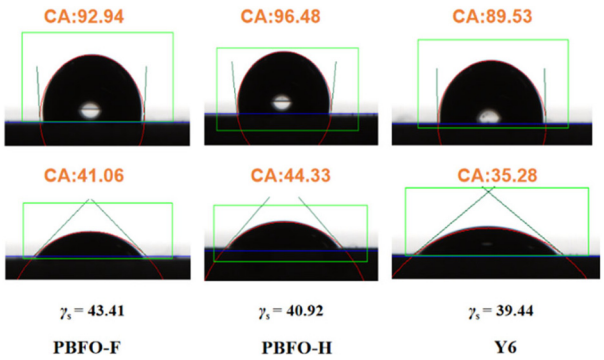

Fig. 5 Contact angles of PBFO-F, PBFO-H, and Y6 neat films with water and diiodomethane.

The transient photocurrent (TPC) technique was used to measure the charge extraction time in order to evaluate the charge extraction rate.[40–42] The TPC curves shown in Fig. 4d evidence that the addition of the fluorine to the polymer backbone helps to decrease the charge extraction time (τ_{ext}) from 0.029 μs in PBFO-H:Y6 to 0.020 μs in PBFO-F which means that there is a faster charge extraction rate in PBFO-F:Y6. Device voltage gradually reduces when there is recombination of holes and electrons.[43] The transient photovoltage (TPV) technique is used to analyze the degree of the charge recombination in the devices, and the plot of the gradual charge decomposition of the TPV analysis translates to the photocarrier lifetimes (τ_{rec}). The value of τ_{rec} was 0.11 μs for both PBFO-H:Y6 and PBFO-F:Y6. The high τ_{rec} value shows that charge recombination is comparatively minimized in the both polymers (Fig. 4e).[44] The TPV decay lifetime is slower than that of the TPC values similar to others in the literature, which confirms the correctness of the results.[45,46] These results confirm that the introduction of fluorine into the polymer is efficient in boosting charge extraction and transfer while reducing charge recombination, and this leads to higher J_{SC} and FF values.

Morphological and packing properties

The miscibility of the donor and acceptor components was derived by measuring the contact angle of each material with water and diiodomethane (Fig. 5). The contact angles were then used to calculate their surface energy values (γ) according to Wu's approach. The γ values were 40.92, 43.41, and 39.44

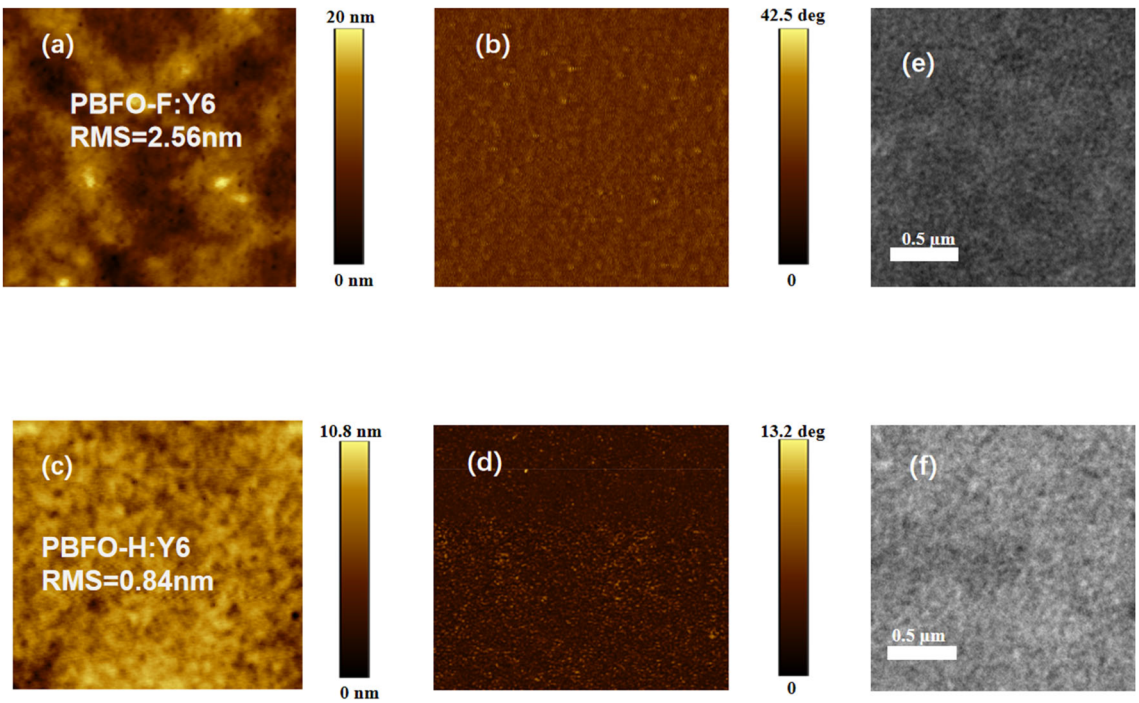

Fig. 6 AFM images (3 × 3 μm) of (a) PBFO-F:Y6 height, (b) PBFO-F:Y6 phase, (c) PBFO-H:Y6 height, and (d) PBFO-H:Y6 phase; TEM images of (e) PBFO-F:Y6 and (f) PBFO-H:Y6.

for PBFO-H, PBFO-F, and Y6 respectively. The Flory–Huggins parameter (χ) which is given by $\chi = \kappa(\sqrt{\gamma_1} - \sqrt{\gamma_2})^2$ is used to determine the miscibility between the polymer and acceptor components. The χ values calculated for the PBFO-F:Y6 blend was $0.095k$ while that of the PBFO-H:Y6 blend was $0.014k$. The smaller χ value of the PBFO-H:Y6 blend shows that there is better miscibility between the two materials. Atomic force microscopy (AFM) was used for investigating the surface morphology of the blend films. As can be seen in Fig. 6(a–d), the root-mean-square (RMS) roughness for the blend films are 2.56 and 0.84 nm for PBFO-F:Y6 and PBFO-H:Y6 respectively. The AFM imagery for PBFO-F:Y6 produces a rough image with conspicuous height variability and its high RMS roughness value indicates that the film has a pronounced topography with peaks and valleys which could be due to material aggregation or phase separation.

Meanwhile, strong aggregation of PBFO-F would probably be induced by its high crystallinity, which would be beneficial for J_{SC} and FF values in devices. PBFO-H:Y6, on the other hand shows a lower RMS roughness value of 0.84 nm which indicates better miscibility with the acceptor. This further confirms the result obtained from the surface energy analysis. The analysis above is further confirmed with transmission electron microscopy (TEM) measurements, with PBFO-F:Y6 showing a rougher surface than PBFO-H:Y6 (Fig. 6e and f). The phase images of the two blends show uniform phase distribution which suggests that both films have no important phase segregation at the nanoscale level of measurement.

Conclusions

In summary, an oxime-functionalized fluorene (FO) was designed and synthesized as an acceptor unit for a D–A donor copolymerized with benzodithiophene (BDT) to construct novel polymers with a wide bandgap of 2.08 eV used with a Y6 acceptor to construct non-fullerene solar cells. Incorporation of fluorine atoms was beneficial for modulating the energy levels of the polymer as well as aggregation behavior and charge mobilities. As a result, the OSC devices based on PBFO-F:Y6 had a maximum PCE of 10.71% with J_{SC}, V_{OC} and E_{loss} approaching state-of-the-art values. These findings give confidence that the novel application of oxime functional groups in D–A donor polymers is promising and a brighter future lies with its further exploration.

Author contributions

Abdullah Adewale Adeoba: polymer synthesis, investigation and writing – original draft. Xiangyu Shen: device fabrication and characterization. Fuzhen Bi: calculation. Jianan Niu: investigation. Mingxin Sun: formal analysis. Shuguang Wen: conceptualization and writing – review & editing. Xichang Bao: analysis, supervision and writing – review & editing.

Data availability

The data supporting this article have been included as part of the ESI.†

Conflicts of interest

There are no conflicts to declare.

Acknowledgements

This work was financially supported by the National Natural Science Foundation of China (no. U1932118 and 52173291), QIBEBT/SEI/QNESL S202305 and OP202309, Shandong Energy Institute (SEIS202108), and Department of Science and Technology of Shandong Province (ZR2020MB085).

Notes and references

1 G. Li, R. Zhu and Y. Yang, *Nat. Photonics*, 2012, **6**, 153–161.
2 H. Sheng, S. Liu, X. Kang, J. Niu, A. A. Adewale, S. Wen, C. Yang, X. Bao and M. Sun, *Nano Energy*, 2024, **126**, 109648.
3 J. Hou, O. Inganäs, R. H. Friend and F. Gao, *Nat. Mater.*, 2018, **17**, 119–128.
4 M. C. Scharber and N. S. Sariciftci, *Prog. Polym. Sci.*, 2013, **38**, 1929–1940.
5 Z. He, C. Zhong, S. Su, M. Xu, H. Wu and Y. Cao, *Nat. Photonics*, 2012, **6**, 591–595.
6 S. Li, C.-Z. Li, M. Shi and H. Chen, *ACS Energy Lett.*, 2020, **5**, 1554–1567.
7 T. H. Lee, S. A. J. Hillman, S. Gonzalez-Carrero, A. Difilippo and J. R. Durrant, *Adv. Energy Mater.*, 2023, **13**, 2300400.
8 L.-Y. Xu, Y. Gao, W. Wang, Y. Shao, M. Chen, X. Yang, Y. Fu, M. Zhang, X. Lu, R. Sun and J. Min, *Energy Environ. Sci.*, 2023, **16**, 3942–3950.
9 Y. Cui, H. Yao, L. Hong, T. Zhang, Y. Xu, K. Xian, B. Gao, J. Qin, J. Zhang, Z. Wei and J. Hou, *Adv. Mater.*, 2019, **31**, 1808356.
10 Y. Ma, Z. Kang and Q. Zheng, *J. Mater. Chem. A*, 2017, **5**, 1860–1872.
11 Y.-W. Su, Y.-C. Lin and K.-H. Wei, *J. Mater. Chem. A*, 2017, **5**, 24051–24075.
12 B. Zheng, L. Huo and Y. Li, *NPG Asia Mater.*, 2020, **12**, 3.
13 K. He, P. Kumar, Y. Yuan and Y. Li, *Mater. Adv.*, 2021, **2**, 115–145.
14 H. Yao, L. Ye, H. Zhang, S. Li, S. Zhang and J. Hou, *Chem. Rev.*, 2016, **116**, 7397–7457.
15 K. He, P. Kumar, Y. Yuan, Z. Zhang, X. Li, H. Liu, J. Wang and Y. Li, *ACS Appl. Mater. Interfaces*, 2021, **13**, 26441–26450.
16 X. Song, Y. Zhang, Y. Li, F. Li, X. Bao, D. Ding, M. Sun and R. Yang, *Macromolecules*, 2017, **50**, 6880–6887.
17 X. Kong, C. Zhu, J. Zhang, L. Meng, S. Qin, J. Zhang, J. Li, Z. Wei and Y. Li, *Energy Environ. Sci.*, 2022, **15**, 2011–2020.

18 B. Pang, C. Liao, X. Xu, L. Yu, R. Li and Q. Peng, *Adv. Mater.*, 2023, **23**, 2300631.
19 J. Wang, Y. Wang, P. Bi, Z. Chen, J. Qiao, J. Li, W. Wang, Z. Zheng, S. Zhang, X. Hao and J. Hou, *Adv. Mater.*, 2023, **35**, 2301583.
20 T. Lin, Y. Hai, Y. Luo, L. Feng, T. Jia, J. Wu, R. Ma, T. A. Dela Peña, Y. Li, Z. Xing, M. Li, M. Wang, B. Xiao, K. S. Wong, S. Liu and G. Li, *Adv. Mater.*, 2024, **36**, 2312311.
21 M. Svensson, F. Zhang, S. C. Veenstra, W. J. H. Verhees, J. C. Hummelen, J. M. Kroon, O. Inganäs and M. R. Andersson, *Adv. Mater.*, 2003, **15**, 988–991.
22 Y.-J. Cheng, S.-H. Yang and C.-S. Hsu, *Chem. Rev.*, 2009, **109**, 5868–5923.
23 D. P. Amit Sharma and W. Tomas, *J. Optoelectron. Adv. Mater.*, 2014, **16**, 1257–1268.
24 M. Sun, L. Wang, Y. Xia, B. Du, R. Liu and Y. Cao, *Front. Chem. Eng. China*, 2008, **2**, 257–264.
25 A. Gadisa, W. Mammo, L. M. Andersson, S. Admassie, F. Zhang, M. R. Andersson and O. Inganäs, *Adv. Funct. Mater.*, 2007, **17**, 3836–3842.
26 M.-H. Chen, J. Hou, Z. Hong, G. Yang, S. Sista, L.-M. Chen and Y. Yang, *Adv. Mater.*, 2009, **21**, 4238–4242.
27 W. Lee, H. Cha, Y. J. Kim, J.-E. Jeong, S. Hwang, C. E. Park and H. Y. Woo, *ACS Appl. Mater. Interfaces*, 2014, **6**, 20510–20518.
28 S. Wen, Y. Li, N. Zheng, I. O. Raji, C. Yang and X. Bao, *J. Mater. Chem. A*, 2020, **8**, 13671–13678.
29 L. Ye, X. Jiao, H. Zhang, S. Li, H. Yao, H. Ade and J. Hou, *Macromolecules*, 2015, **48**, 7156–7163.
30 K. He, P. Kumar, M. Abd-Ellah, H. Liu, X. Li, Z. Zhang, J. Wang and Y. Li, *Macromolecules*, 2020, **53**, 8796–8808.
31 D. Zhu, Q. Zhu, C. Gu, D. Ouyang, M. Qiu, X. Bao and R. Yang, *Macromolecules*, 2016, **49**, 5788–5795.
32 B. Aldo, B. Simone, G. Giambattista, L. Annalina, E. O. Susanna Nencettia, R. Simona, R. Armando and G. Soldanib, *Eur. J. Med. Chem.*, 2001, **36**, 799–807.
33 A. Jessie, D. A. P. Blake, L. Shuqiong, C. J. Walton, M. Peter and K. U. Ingold, *J. Org. Chem.*, 2004, **69**, 3112–3120.
34 H. Sun, T. Liu, J. Yu, T.-K. Lau, G. Zhang, Y. Zhang, M. Su, Y. Tang, R. Ma, B. Liu, J. Liang, K. Feng, X. Lu, X. Guo, F. Gao and H. Yan, *Energy Environ. Sci.*, 2019, **12**, 3328–3337.
35 P. Chao, M. Guo, Y. Zhu, H. Chen, M. Pu, H.-H. Huang, H. Meng, C. Yang and F. He, *Macromolecules*, 2020, **53**, 2893–2901.
36 Y. Xie, W. Wang, W. Huang, F. Lin, T. Li, S. Liu, X. Zhan, Y. Liang, C. Gao, H. Wu and Y. Cao, *Energy Environ. Sci.*, 2019, **12**, 3556–3566.
37 J.-L. Wu, F.-C. Chen, Y.-S. Hsiao, F.-C. Chien, P. Chen, C.-H. Kuo, M. H. Huang and C.-S. Hsu, *ACS Nano*, 2011, **5**, 959–967.
38 L. J. A. Koster, V. D. Mihailetchi, R. Ramaker and P. W. M. Blom, *Appl. Phys. Lett.*, 2005, **86**, 123509.
39 D. Liu, C. Gu, J. Wang, D. Zhu, Y. Li, X. Bao and R. Yang, *J. Mater. Chem. A*, 2017, **5**, 9141–9147.
40 J. Wang, M. Zhang, J. Lin, Z. Zheng, L. Zhu, P. Bi, H. Liang, X. Guo, J. Wu, Y. Wang, L. Yu, J. Li, J. Lv, X. Liu, F. Liu, J. Hou and Y. Li, *Energy Environ. Sci.*, 2022, **15**, 1585–1593.
41 X. Liu, R. Tian, Z. Xiong, Y. Liu and Y. Zhou, *Chin. Opt. Lett.*, 2023, **21**, 120031.
42 X. Kong, C. Zhu, J. Zhang, L. Meng, S. Qin, J. Zhang, J. Li, Z. Wei and Y. Li, *Energy Environ. Sci.*, 2022, **15**, 2011–2020.
43 S. Chen, Y. Liu, L. Zhang, P. C. Y. Chow, Z. Wang, G. Zhang, W. Ma and H. Yan, *J. Am. Chem. Soc.*, 2017, **139**, 6298–6301.
44 Y. Cheng, B. Huang, X. Huang, L. Zhan, S. Kim, Q. Xie, C. Liu, T. Heumüller, Z. Liu, Y. Zhang, F. Wu and C. Yang, *Angew. Chem., Int. Ed.*, 2022, **61**, e202200329.
45 H. Aldosari, J. Jurado, K. Alkhezaim, S. Alam and F. Laquai, *ACS Appl. Energy Mater.*, 2024, **7**(16), 7055–7063.
46 Y. Yan, X. Zhou, F. Zhang, J. Zhou, T. Lin, Ya. Zhu, D. Xu, X. Ma, Y. Zou and X. Li, *J. Mater. Chem. A*, 2022, **10**, 23124–23133.